J Electroceram (2007) 19:387–393
DOI 10.1007/s10832-007-9034-5

A simple and powerful analytical model for MEMS piezoelectric multimorphs

W. E. Booij · A. H. Vogl · D. T. Wang · F. Tyholdt · N. P. Østbø · H. Ræder · K. Prume

Received: 17 March 2006 / Accepted: 9 November 2006 / Published online: 13 March 2007

Abstract We have developed an analytical model for use in design and modelling of piezoelectric MEMS devices. The model allows for incorporation of any number of device material layers in a multimorph structure including piezoelectric materials. The resulting lumped circuit model fully incorporates the electro-mechanical coupling effects in the piezoelectric layers as well as electrical or mechanical loading of the device structure. Since the model is analytic, and only requires the specification of well-defined material properties, it allows for fast and interactive modelling of a multitude of MEMS device structures incorporating piezoelectric materials. We will demonstrate the capability of the model by presenting results from fitting the model to impedance measurements performed on cantilever structures. This allows for extraction of device and material parameters that are difficult to obtain by other means, such as the piezoelectric coefficient and the mechanical quality factor.

Keywords Multimorph cantilever · Piezoelectric · Analytical model · MEMS · Energy harvesting

1 Introduction

The integration of piezoelectric thin films in micro electro-mechanical systems (MEMS) has recently gained increased impetus due to the interest in energy harvesting from vibration sources for autonomous sensors. However, the span of application areas of such piezoelectric devices is much wider and encompasses micropumps, micro-optics, inertial devices, microphones, ultrasonic transceivers and acoustic wave filters. It is interesting to note that these applications range in frequency from close to DC up to several GHz. The process technology to integrate high quality piezoelectric thin films in MEMS is maturing fast, with volume production now possible for both PZT and AlN thin films. We believe that low cost piezoelectric MEMS devices will soon be a reality based on recent results on PZT thin films deposited using sol-gel technology. This technology has been developed in close collaboration with P. Muralt and collaborators at EPFL, Lausanne, Switzerland [2, 4, 5, 7, 8, 12] through the European Framework 6 CRAFT project MEMS-pie [11, http://www.sintef.no/mems-pie]. The project is on route to establish a capable foundry process for piezoelectric devices.

In order to be able to support such a process with a capable design and characterisation service we have developed a simple but powerful dynamic model for a piezoelectric multimorph. In its current form the model is focused on the well-known MEMS workhorse, the cantilever. However, the formalism detailed below can be extended to other structures with relative ease.

2 System description

The aim of the model is to be able to aid the design and characterisation of MEMS cantilever structures, based on a SOI process. This process can both include PZT and AlN thin films. Currently a film thickness of 2 μm is used and the design exploits the transversal (31) mode of the piezo-

W. E. Booij · A. H. Vogl (✉) · D. T. Wang · F. Tyholdt · N. P. Østbø · H. Ræder
SINTEF, P. O. Box 124 Blindern, 0314 Oslo, Norway
e-mail: Andreas.Vogl@sintef.no

K. Prume
aixACCT Systems GmbH, Dennewartstr. 25-27, 52068 Aachen, Germany

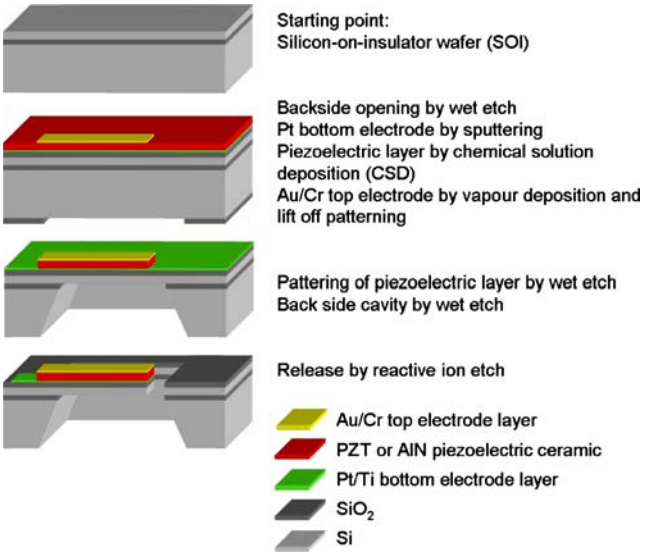

Fig. 1 Schematic overview of the SOI based process for the fabrication of piezoelectric devices (from [11])

electric thin film. Both membrane and cantilevers structures incorporating bulk masses can be fabricated using the process described schematically in Fig. 1.

To obtain exact transfer functions of the system described in Fig. 2 one needs to use all the eigenmodes of the cantilever. For each mode one must calculate the mode effective mass, the mode stiffness, the coupling to the input stress and the coupling to the output signal.

Ideally we could use the lowest true eigenmode to construct a simplified transfer function [3]. However, for a cantilever the lowest eigenmode has a non-trivial mathematical expression for the shape and for simplicity we use the deflection shape under static conditions, i.e. constant curvature (κ), as a "test function" to approximate the lowest eigenmode in the spirit of the Rayleigh–Ritz procedure [13]. With this formalism we can write the shape of the bending line as a function of time and the x-coordinate (Fig. 2) of the cantilever:

$$\upsilon(x,t) = \kappa_0 \cdot e^{j\omega t} \cdot \frac{x^2}{2} \tag{1}$$

In the mechanical domain curvature κ and moment (M) are the independent system variables. In the electrical domain we have selected charge (q) and voltage (V) as the independent variables. This selection of variables allows us to directly use the expressions of [15]. Weinberg arrived at simple expression for the following parameters that govern the static deformation of a piezoelectric multimorph:

C_M the curvature per unit torque
M_V the torque per unit voltage across the electrodes
C_P the capacitance of the piezoelectric layers

Using these parameters, we arrive at the following coupled system equation for the system [6]:

$$\begin{aligned} m \cdot \ddot{\kappa} + \gamma \cdot \dot{\kappa} + \frac{1}{C_M} \cdot \kappa - k_{\mathrm{me1}} V &= M_{\mathrm{ext}}(t) \\ \dot{q} - k_{\mathrm{me2}} \dot{\kappa} - C_p \dot{V} - \frac{V}{R_P} &= 0 \end{aligned} \tag{2}$$

Where m, γ are the modal mass and modal mechanical damping coefficient, k_{me1} the modal coefficient for piezoelectric the torque per unit voltage, M_{ext} the externally applied torque (sensor mode), k_{me2} the modal coefficient for the piezoelectric charge per unit curvature, R_P the equivalent parallel resistance associated with the losses in the piezoelectric and Q_{ext} the externally supplied charge (actuator mode). We can immediately identify that $k_{\mathrm{me1}}=M_V$ and that due to the choice of system variables $k_{\mathrm{me1}} \neq k_{\mathrm{me2}}$. We can identify k_{me2} by equating the total power delivered by an applied voltage in the electrical system to the power delivered to the mechanical system by the resulting moment. The power resulting from the piezoelectric moment can be calculated from the product of a uniform force per length unit $F_1 = M_V V / L^2$ and the local velocity on a segment dx along the cantilever:

$$\begin{aligned} V \cdot \frac{\mathrm{d}q}{\mathrm{d}t} = V \cdot k_{\mathrm{me2}} \cdot \dot{\kappa} &= \int_0^L \frac{M_V V}{L^2} \frac{1}{2} \dot{\kappa} x^2 \mathrm{d}x \\ &= \frac{M_V V \cdot \dot{\kappa} \cdot L}{6} \end{aligned} \tag{3}$$

and therefore $k_{\mathrm{me2}} = M_V L/6$.

The only remaining unknown parameter, the modal mass can be derived from the eigenfrequency through equating the maximum potential and the maximum kinetic energy and solving for ω_0 [13]:

$$\omega_0^2 = \frac{\frac{1}{2}\kappa^2 \cdot \frac{1}{C_M} \cdot L}{\frac{1}{2}\kappa^2 \cdot m_l \cdot \frac{L^5}{20}} = \frac{\frac{1}{C_M}}{m_l \cdot \frac{L^4}{20}} = \frac{k}{m} \tag{4}$$

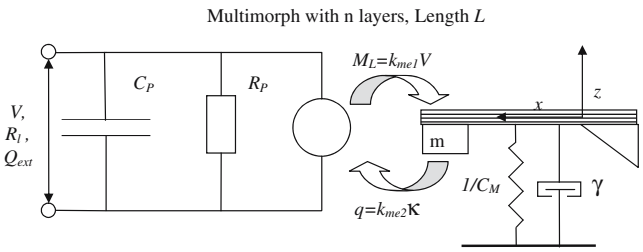

Fig. 2 Schematic lumped circuit model representation of the piezoelectric cantilever structure

and so $m = m_l \cdot \frac{L^4}{20}$ where m_l is the mass per length unit:

$$m_l = w \cdot \sum_{i=1}^{n} \rho_i \cdot t_i \tag{5}$$

where w is the cantilever width, ρ_i and t_i, respectively, the mass density and thickness of layer i.

The most important disadvantage of using the constant curvature as the mode shape is that the eigenfrequency is significantly overestimated when compared to the eigenfrequency calculated from the more correct mode shape [9]:

$$\omega_0^2 = \frac{(1.8751)^4}{C_M \cdot m_l \cdot L^4} \tag{6}$$

The constant curvature mode shape approach results in a first eigenmode frequency estimate that is 27% higher than that of the more correct expression (6). However, in comparison with other models, this model based on the constant curvature approximation offers the advantage of resulting in simple algebraic expressions for device transfer functions. This means that the model can be applied in device characterisation and process control situations, where computer processing time is scarce.

3 Sensor transfer functions

We can derive the transfer function in sensor mode from Eq. (2) by including a load on the electrical side. If we take the load to be purely resistive (R_L) we obtain the following additional relation between charge and voltage:

$$V = -R_L \cdot \dot{q} \tag{7}$$

Using this in conjunction with both the electrical and mechanical system equations (2), we can derive the following transfer functions that fully describe the system behaviour:

$$H_{\kappa q}(\omega) = \frac{\kappa(\omega)}{q(\omega)} = \frac{C_P}{k_{me2}}\left(\frac{1}{C_P} + \frac{R_L}{R_P C_P} + j\omega R_L\right)$$
$$H_{M\kappa}(\omega) = \frac{M_{ext}(\omega)}{\kappa(\omega)} = -m\omega^2 + j\omega\gamma + \frac{1}{C_M} + \frac{j\omega \cdot k_{me1} R_L}{H_{\kappa q}(\omega)} \tag{8}$$

The reciprocal of the last equation for example relates curvature and the applied external moment. In most cases we are interested in the charge resulting from an external mechanical moment. In this case we are interested in the following transfer function:

$$H_{qM}(\omega) = \frac{q(\omega)}{M(\omega)} = \frac{1}{H_{M\kappa}(\omega) \cdot H_{\kappa q}(\omega)} \tag{9}$$

4 Energy harvester

An energy harvesting device based on a piezoelectric multimorph cantilever can be treated as a sensor mode device as described by Eq. 8. However, for energy harvesting applications we are interested in deriving an expression for both the voltage across and power dissipated in the load resistor as a function of applied acceleration. Using Eqs. 7 and 8 we can express the transfer function for the generated voltage as a result of an input moment as:

$$H_{VM}(\omega) = H_{Vq}(\omega) \cdot H_{qM}(\omega) = H_{Vq}(\omega) \cdot \left(H_{\kappa q}(\omega) \cdot H_{M\kappa}(\omega)\right)^{-1} = \\ = -j\omega \cdot R_L \left(H_{\kappa q}(\omega) \cdot H_{M\kappa}(\omega)\right)^{-1} \tag{10}$$

We now only need to find the relation between the acceleration applied to the cantilever ($a_N(t)$) normal to its surface and the resulting moment (assuming the cantilever is homogenous along its length):

$$M_{\text{ext}} = \int_{x=0}^{L} \mathrm{d}M_{\text{ext}} = \int_{x=0}^{L} F_l \cdot x \cdot \mathrm{d}x = \int_{x=0}^{L} m_l \cdot a_N \cdot x \cdot \mathrm{d}x = m_l \cdot a_N \cdot \frac{L^2}{2} \tag{11}$$

From Eqs. 10 and 11 we can calculate the voltage across the load resulting from an input acceleration:

$$V(\omega) = H_{VM} \cdot M_{ext}(\omega) = H_{VM} \cdot m_l \cdot \frac{L^2}{2} \cdot a_N(\omega) \tag{12}$$

The resulting power transferred to the load is then given by:

$$P(\omega) = \frac{V(\omega)^2}{R_L} = \left(m_l \cdot \frac{L^2}{2}\right)^2 \cdot \frac{|H_{VM} a_N(\omega)|}{R_L} \tag{13}$$

Another important figure of merit for an energy harvesting device is the ratio of the energy stored in the electrical

Table 1 Material parameters and film thicknesses as used in the modelling work in this paper.

Material	Thickness (nm)	Young's modulus (GPa)	Poisson ratio	Mass density (kg/m^3)
Si	9,000	166	0.065	2,330
SiO_2	1,333	70	0.3	2,200
Pt	120	168	0.38	21,090
PZT	2,000	61	0.28	7,750
Au/Cr (Au)	250	78	0.42	19,300

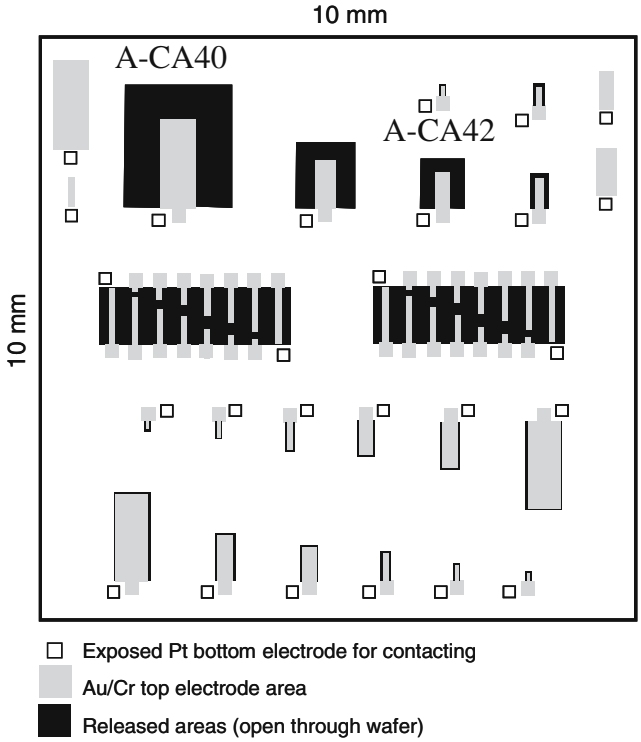

Fig. 3 Schematic design layout of a 10×10 mm square dedicated to catilevers. Designs with both narrow (5 and 10 μm) and wide (equal to cantilever width) clearings were included

domain over the energy stored in the mechanical domain (k_{eff}^2). This ratio can be shown to be:

$$k_{\text{eff}}^2 = \frac{C_M k_{\text{me1}} k_{\text{me2}}}{C_P} \tag{14}$$

5 Actuator transfer functions

To derive the actuator transfer functions we set $M_{\text{ext}}(t)=0$ and set $q=Q_{\text{ext}}(t)$. We are particularly interested in deriving the relation for the actuator impedance, since this can be easily related to experiments. The method is well established for piezoelectric unimorphs [1]. Instead of the impedance $Z(\omega)$, we use the admittance $Y(\omega)$ since this results in simpler expressions:

$$Y(\omega) = \frac{1}{Z(\omega)} = \frac{I(\omega)}{V(\omega)} = \frac{j\omega \cdot Q_{\text{ext}}(\omega)}{V(\omega)}$$
$$= \frac{1}{R_P} + j\omega C_P + \frac{j\omega \cdot k_{\text{me1}} \cdot k_{\text{me2}}}{-m\omega^2 + j\omega\gamma + \frac{1}{C_M}} \tag{15}$$

6 Material parameters and dimensions used in the model

To obtain good agreement between modelling results and experiments it is essential to use accurate values for material parameters and dimensions. However, accurate material parameters often do not exist for thin films. Hence, we have relied on bulk values from literature [15], see Table 1. The materials are listed in bottom to top order as fabricated in the process described in Fig. 1.

The electrical properties of PZT thin films are on the other hand well-known and they are also in addition easily measured on individual devices. Thus, for the calculations we have used a relative dielectric constant (ε_r) of 1,132±51 and a loss factor of 0.029±0.003. These average and standard deviation values were obtained from $C(V)$ measurements on more than 150 devices distributed on the same wafer which was also used for the impedance measurements shown later. The generally accepted value for the effective transversal piezoelectric charge coefficient of a deflected multimorph, $e_{31,f}$ in {100} oriented sol-gel PZT is ~−12 C/m^2 [5]. In the expression for M_V (torque per

Table 2 Length, width and resonance frequencies for the MEMS-pie cantilever devices.

Length (μm)	Width (μm)	f_{me} (kHz)	F_{m} (kHz)
150	30	674	515
300	60	169	129
500	100	61	46.4
600	240	42	32.2
800	320	23.7	18.1
1 500	600	6.74	5.15

Table 3 Fitting parameters and resulting model parameters for the device A-CA40 and A-CA42.

Fit parameters	Model parameters
A-CA40:	
Q_m=115	M_V=−4.236·10^{-8}C
d_{31}=1.4·10^{-10} C·N^{-1}	C_m=8.375·10^7 s^2/(kg·m^3)
ε_r=890	C_p=3.679·10^{-9} F
tan δ=0.2	m=14.686 kg·μm^3
L=1.595·10^3 μm	f_m=4.538 kHz
w=600 μm	K_{eff}^2 = 0.011
A-CA42:	
Q_m=85	M_V=1.695·10^{-8}C
d_{31}=−1.4·10^{-10} C·N^{-1}	C_m=2.094·10^8 s^2/(kg·m^3)
ε_r=1,030	C_p=8.413·10^{-10} F
tan δ=0.12	m=0.214 kg·μm^3
L=697 μm	f_m=23.762 kHz
w=240 μm	K_{eff}^2 = 8.301 · 10^{-3}

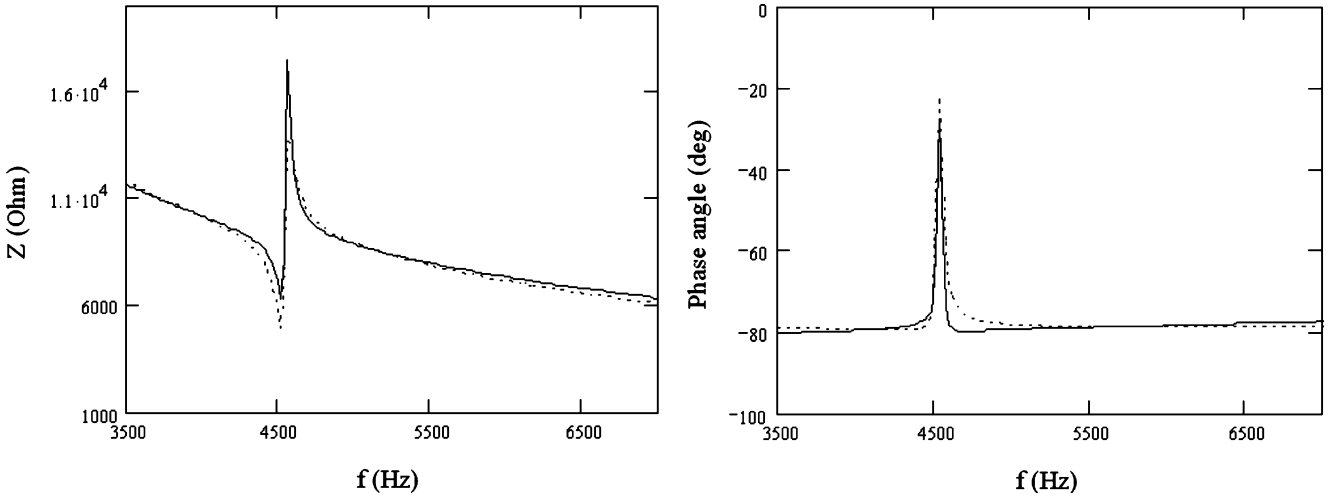

Fig. 4 Magnitude and phase angle of the impedance of device A–CA40. The *continuous line* are the measurements, whereas the *dotted lines* represent the model results

unit voltage) Weinberg [15] uses d_{31} which is related to $e_{31,f}$ in the following way [15]:

$$e_{31,f} = \frac{d_{31} \cdot E}{1 - v_c} \tag{16}$$

where E is the Youngs modulus and v_c the Poisson ratio of PZT.

The MEMS-pie test wafer contains a large number of different tests structures. However, in this work we focus on the die that contains cantilever structures, shown in Fig. 3. All the cantilevers, having individual backside cavities, where designed with a specific length to width aspect ratio of 2.5 or 5. The lengths and widths are shown in Table 2 together with the resonance frequency f_m (calculated from Eq. 6) and f_{me} which was calculated using the model described here. Note that f_{me} is almost 31% higher than f_m, of which 27% is due to the different mode shape as discussed earlier and the remaining 4% due to an increase in stiffness from electromechanical coupling in the piezoelectric material. For the sensor mode operation we have used an electrical load of 1 MΩ. (Table 3)

7 Fitting actuated cantilevers

We obtained impedance measurements on selected cantilever structures shown in Fig. 3 that were fitted to the actuator model discussed, with the aim of verifying the model and extracting material parameters that are otherwise difficult to obtain such as the mechanical quality factor

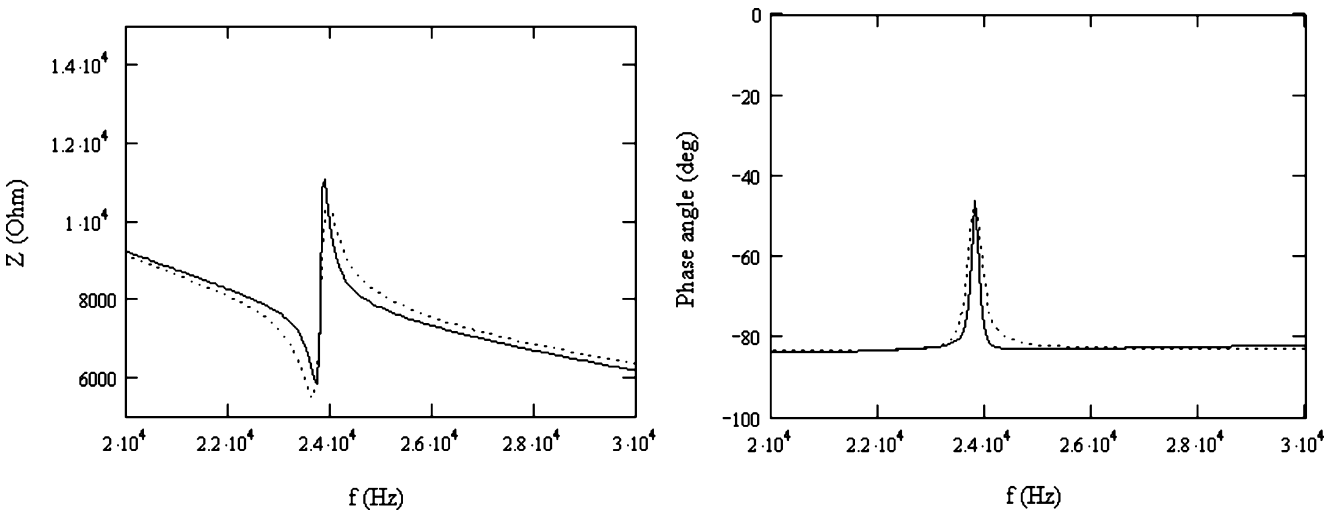

Fig. 5 Magnitude and phase angle of the impedance of device A–CA42. The *continuous line* are the measurements, whereas the *dotted lines* represent the model results

(Q_m) and $d_{31}Q_m$ is related to the mechanical damping coefficient γ in the following way:

$$Q_m = \frac{\sqrt{\frac{m_l}{C_m}}}{\gamma} \tag{17}$$

To deal with the error introduced in the eigenmode frequency by the constant curvature approach, we have introduced a correction factor for m so that the model eigenmode matches the expected value of Eq. 6:

$$c_m = \frac{20}{1.8751^4} = 1.618 \tag{18}$$

To obtain a fit we used five adjustable parameters: d_{31}, Q_m,ε_r, tan δ (loss factor) and the cantilever length L. The selection of the cantilever length as an adjustable parameter makes good sense because of two factors related to the wet etch process used to define the backside cavity: a) The wet etch process is prone to give a large underetch (10% of etch depth) that also varies on the wafer. b) The sloped side wall profile resulting from of the wet etch process can result in an increase of the effective length of the cantilever due to flexing of the cantilever anchoring.

Impedance measurements were obtained using an Aix-ACCT TF2000 analyzer. The results from the impedance measurements for two of the devices from the die shown in Fig. 3 were fitted to the actuator model described. The fitting was done qualitatively using starting values from other electrical measurements (for example tan δ and ε_r) as well as design values (for L). The only truly free parameter for the fit was Q_m Although there is no unique solution for such a fit, the fitted parameters have a very distinct effect on the shape of the impedance curves. A fully automatic routine for fitting data should therefore be possible as long as suitable initial and boundary values for the fitted parameters are taken into account in the optimisation process. For device A-CA-40 the model and measurements match very well using fit parameters that are within the expected range. However, ε_r, is lower than expected whereas tan δ is almost a factor 10 higher than obtained in earlier $C(V)$ measurements on the same device.The reason for these discrepancies can most likely be attributed to the poor quality of the probe contact to the bottom Pt electrode, which adds a significant series resistance to the electrical system which is not included in the model. For device A-CA42 the contact problem is not as manifest judged from the values of tan δ.From the fitted d_{31} value we can calculate $e_{31,f}$ using Eq. 16 resulting in $e_{31,f}$=−11.86 C/m^2, which agrees well with $e_{31,f}$ values obtained using four point bending measurements (AixACCT TF2000 analyzer [10]) on the same batch of sol-gel thin films (−14 C/m^2 to −15 C/m^2) [14]. It can be seen that the length of the cantilevers in both cases is 95–97 μm longer than the design length, which agrees reasonably well with the observed undercut resulting from the wet etch. (Figs. 4 and 5)

8 Conclusions

A complete dynamic model for a piezoelectric cantilever was presented that allows for accurate prediction of device characteristics. The model uses the simplest possible mode shape for the deformation of the cantilever (constant curvature) and results in simple algebraic expressions for the transfer functions that govern the dynamic behaviour of the cantilever. Subsequently, the model is very useful in the design of various devices based on piezoelectric actuated cantilevers. In addition, expressions for sensor, actuator and energy harvesting mode of operation have been derived. The expressions for the actuator mode of operation where fitted to impedance measurement results obtained from two cantilever devices. Utilising the model we were able to extract five device and material related parameters; d_{31}, Q_m,ε_r, tan δ and the cantilever length L from a single impedance scan measurement. The simplicity of the model means that these parameters can be extracted automatically using a general fit routine as part of an automated characterisation setup.

The most important shortcoming of the mode shape simplification applied in this paper is the large error in the predicted resonance frequency. For applications demanding higher accuracy than the current approach can deliver, the reader is referred to DuToit [3], who recently published a similar theoretical approach focussed on energy harvesting devices using more correct mode shapes.

Acknowledgements The authors acknowledge the support from the European Commission through the MEMS-pie project (Contract no. COOP-CT-2004-508219) [http://www.sintef.no/mems-pie] and contributions from the companies involved: aixACCT Systems GmbH (DE), Hök Instrument AB (SE), Noliac A/S (DK), Precision Acoustics Ltd. (UK) and Sonitor AS (NO).

References

1. M. Alguero, C. Alemany, L. Pardo, A.M. Gonzalez, J. Am. Ceram. Soc. **87**, 209–215 (2004)
2. M.A. Dubois, P. Muralt, D.V. Taylor, S. Hiboux, Integr. Ferroelectr. **22**, 1055 (1998)
3. N.E. duToit, B.L. Wardle, S.-G. Kim, Integr. Ferroelectr. **71**, 121 (2005)
4. N. Ledermann, P. Muralt, J. Baborowski, M. Forster, J.-P. Pellaux, J. Micromechanics Microengineering 1650 (2004)
5. N. Ledermann, P. Muralt, J. Baborowski, S. Gentil, Kapil Mukati, M. Cantoni, A. Seifert, N. Setter, Sens. Actuators A **105**, 162 (2003)
6. F. Lu, H.P. Lee, S.P. Lim, Smart Mater. Struct. **13**, 57 (2004)
7. P. Muralt, J. Micromechanics Microengineering **10**, 136 (2000)

8. P. Muralt, IEEE Trans. Ultrason. Ferroelectr. Freq. Control **47**, 903 (2000)
9. C.H. Nguyen, S.J. Pietrzko, Mech. Syst. Signal Process. **18**, 929 (2004)
10. K. Prume, P. Muralt, F. Calame, T. Schmitz-Kempen, S. Tiedke, IEEE Trans. Ultrason. Ferroelectr. Freq. Control **54**, 8 (2007)
11. H. Ræder, F. Tyholdt, W. Booij, F. Calame, N.P. Østbø, R. Bredesen, K. Prume, G. Rijnders, P. Muralt, J. Electroceram. in press (2007)
12. A. Seifert, N. Ledermann, S. Hiboux, J. Baborowski, P. Muralt, N. Setter, Integr. Ferroelectr. **35**, 159 (2001)
13. S.D. Senturia, *Microsystem Design* (Kluwer, Boston, 2001), pp. 260–264
14. F. Tyholdt, F. Calame, K. Prume, W. Booij, H. Ræder, P. Muralt, J. Electroceram. in press (2007)
15. M.S. Weinberg, (ASME/IEEE) Journal of MEMS **8**, 529–533 (1999)